*Combustion, Explosion, and Shock Waves, Vol. 45, No. 4, pp. 461–477, 2009*

# Mechanism of HMX Combustion in a Wide Range of Pressures

**V. P. Sinditskii,[1] V. Yu. Egorshev,[1] M. V. Berezin,[1] and V. V. Serushkin[1]**

UDC 536.45

Translated from *Fizika Goreniya i Vzryva*, Vol. 45, No. 4, pp. 128–146, July–August, 2009.
Original article submitted October 25, 2008.

**Data obtained in the present work and available publications on combustion of cyclotetramethylene tetranitramine (HMX) at different initial temperatures are analyzed. The temperature sensitivity of the HMX burning rate is demonstrated to increase with increasing initial temperature at pressures of 0.1 to 10 MPa, which is typical for combustion of substances with the leading reaction in the condensed phase (c-phase model). Experimental values of the temperature sensitivity of the burning rate in the pressure interval between 0.1 and 1 MPa are higher than the values predicted by the c-phase model, but this fact indicates the transition of the combustion process to another regime rather than the combustion instability in this area. The flame structure of burning HMX with different additives is studied with the help of thin tungsten–rhenium thermocouples in the pressure range from 0.025 to 1 MPa. The gas-phase flame is found to ignite in an inductive mode, at least up to a pressure of 1 MPa. The surface temperature is obtained as a function of pressure on the basis of experimental data in a wide range of pressures: $\ln p = -14{,}092/T + 21.72$ ($p$ in atm). Two possible reasons for the oscillatory regime of HMX combustion observed at atmospheric pressure are proposed: the emergence of resonance phenomena during combustion of an inhomogeneous gas mixture in the tube and the lack of correspondence between the chemical reaction rate in the gas phase at the instant of the resonance and its energy capabilities, which do not allow a necessary HMX gasification rate to be ensured. A mechanism of HMX combustion is proposed, which offers an adequate description in a wide range of pressures up to 10 MPa. The mechanism is based on the leading role of HMX decomposition in the melt at the surface temperature.**

**Key words: HMX, combustion mechanism, temperature sensitivity, burning rate, flame structure, kinetics of heat release in the condensed phase.**

## INTRODUCTION

Combustion of cyclotetramethylene tetranitramine (HMX) has been intensely studied since the 1970s [1–16] when nitramines possessing high densities and high energy characteristics gained applications as components of modern rocket propellants. Despite almost 40-year investigations, however, there is still no common understanding of the HMX combustion mechanism, which is evidenced by the recent discussion in Combustion, Explosion, and Shock Waves [17–19].

The primary open question is the relative contributions of condensed-phase reactions at high and low pressures. In early publications [1–4], the major part of HMX was assumed to decompose in the gas phase. Mitani and Williams [5] proposed a mechanism of HMX combustion, which implied that 35% of the substance decompose in the melted layer on the surface at atmospheric pressure and 25% decompose at a pressure $p = 10$ MPa; the contribution of the gas phase to the heat content of the condensed phase changes from 10

[1]Mendeleev University of Chemical Technology of Russia, Moscow 125047; vps@rctu.ru.

0010-5082/09/4504-0461 © 2009 Springer Science + Business Media, Inc.

to 50%. On the basis of microthermocouple measurements, Kubota and Sakamoto [12] and Lengelle et al. [20] concluded that reactions proceeding both in the condensed phase and in the flame make the determining contribution to the HMX burning rate. Prasad et al. [10] proposed a mechanism of HMX combustion, which implied that 57% of the substance decompose in the condensed phase at atmospheric pressure and a complete transition to the gas-phase model of combustion occurred at $p = 9$ MPa.

An opposite conclusion was drawn in [13–15]: at atmospheric and subatmospheric pressures, the heat balance on the HMX surface obtained by thermocouple measurements testifies that the condensed phase (c-phase) is heated and evaporates mainly at the expense of heat incoming from the gas phase. As the pressure increases, however, the condensed-phase reactions become responsible for the burning rate. The three-phase (solid, liquid, and gas phases) model of HMX combustion [9] offers an adequate description of experimental data obtained by thermocouples [13–15]; the leading role in this model, however, is given to gas-phase reactions not only at atmospheric pressure, but at high pressures as well.

Studying combustion at different initial temperatures is helpful in understanding the mechanism of combustion of energetic materials. The fact is that the dependence of the burning rate on the initial temperature $\ln u(T_0)$ and the dependence of the temperature sensitivity of the burning rate on the initial temperature $\beta(T_0)$ are substantially different in two basic models of combustion. In the gas-phase combustion model proposed by Belyaev and Zel'dovich [21, 22], the burning rate as a function of $T_0$ is described by the relation $u = A\exp(-E/2RT_f)$; in the coordinates $\ln u$ and $T_0$, this dependence is an upward convex curve. In the combustion model with the leading reaction in the condensed phase (c-phase model) [22], the function $u(T_0)$ is expressed as $u = A/(T_s - T_0)$; in the coordinates $\ln u$ and $T_0$, this function is a downward convex curve. The difference in the dependences $\beta(T_0)$ is even more noticeable: in the gas-phase model, the temperature sensitivity is described by the formula $\beta = E/2RT_f^2$ and decreases with increasing initial temperature; in the c-phase model, the temperature sensitivity is described by the formula $\beta = 1/(T_s - T_0)$ and increases with increasing initial temperature. (In these formulas, $E$ is the activation energy, $T_f$ is the flame temperature, $T_s$ is the surface temperature, and $A$ is a constant.)

The goal of the present activities was to find the HMX combustion mechanism in a wide range of pressures. For this purpose, we examined the flame structure of HMX with various additives in the pressure range from 0.025 to 1 MPa with the use of thin tungsten–rhenium thermocouples, studied HMX combustion at different initial temperatures and at pressures of 0.1, 0.2, 0.5, and 1 MPa, and performed a coupled analysis of data obtained in the present work and available publications on HMX combustion, temperature sensitivity of HMX combustion, and temperature distribution in the combustion wave at different pressures.

## EXPERIMENTAL PART

HMX combustion in nitrogen in a 1.5-liter BPD-400 constant-pressure bomb was studied. At pressures below the atmospheric value, HMX combustion was studied in a 40-liter evacuated chamber equipped with a vacuum gauge. To avoid the influence of oxygen contained in air on the combustion process after strand installation, the chamber was blown with nitrogen. Cylindrical pressed samples with the mean density of 1.76 g/cm$^3$ and diameters of 7 mm ($p = 1$ and 0.5 MPa) and 10 mm ($p = 0.1$ MPa and subatmospheric pressures) were used. To prevent flame propagation along the side surface, the strands were inhibited by epoxy resin coatings, with further solidification inside Plexiglas tubes with a 12-mm inner diameter. In some experiments, the strands were clad with a transparent adhesive tape. The burning rate was determined by video recording the process.

The temperature profiles in the combustion wave were measured by flat U-shaped tungsten–rhenium microthermocouples with the junction thickness of 5–7 $\mu$m (the thermocouple width was 80–100 $\mu$m, and the arm length was $\approx$1 mm). The influence of the initial temperature on the burning rate was studied in a constant-pressure device equipped with a thermostat. The thermostat was a massive copper block with a window for combustion observations and with a cylindrical channel where the strand was located. The copper block was heated by the Peltier element, and the temperature was monitored with the use of a Chromel–Copel thermocouple.

Thermodynamic calculations were performed by the REAL code [23].

## RESULTS AND DISCUSSION

### HMX Burning Rate Versus Pressure

One of the most important characteristics of combustion of energetic materials is the dependence of

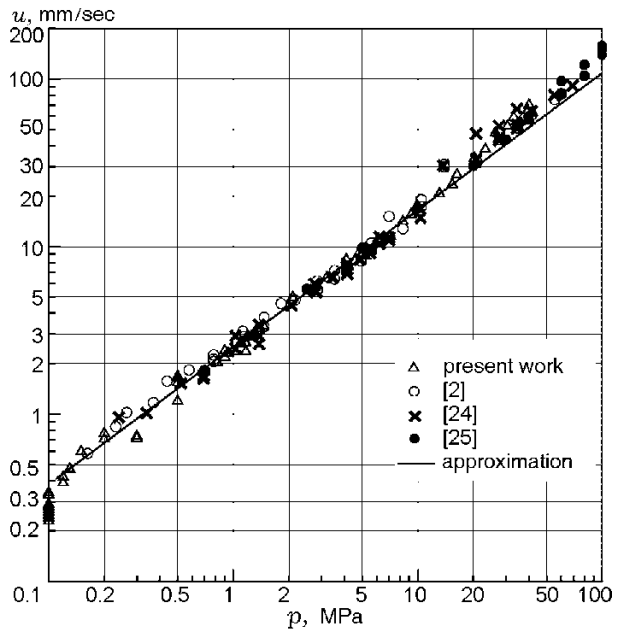


**Fig. 1.** HMX burning rate versus pressure.

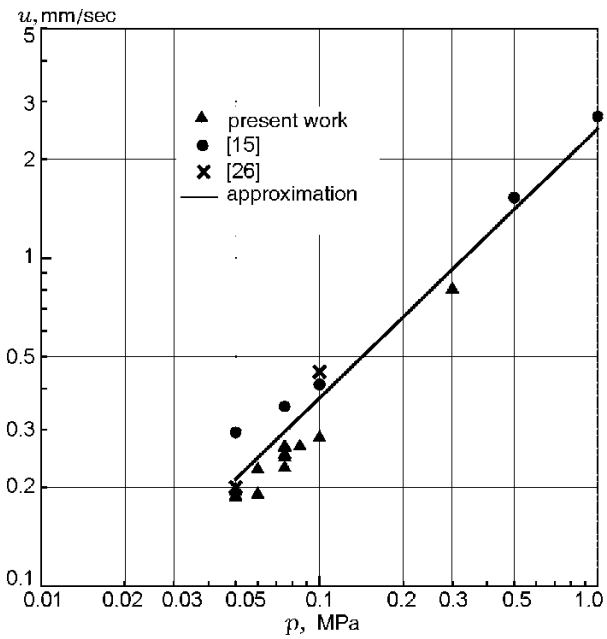


**Fig. 2.** HMX burning rate at low pressures.

the burning rate on pressure. Figure 1 shows the most detailed and, in our opinion, reliable data on HMX combustion obtained in a wide range of pressures. These are results of American researchers [2, 24] (obtained in 1979 and 1999, respectively), results of Glazkova [25] (obtained at the Institute of Chemical Physics of the Academy of Sciences of the USSR in the 1970–1980s), and results obtained at the Mendeleev University of Chemical Technology of Russia (obtained since the 1970s up to now). HMX combustion under similar conditions was considered in all these investigations: strands 6–7 mm in diameter, their density being 1.72–1.76 g/cm$^3$. As is seen in Fig, 1, the HMX burning rates obtained in different laboratories are in good agreement, and the curve $u(p)$ has an inflection at $p = 13$–$15$ MPa. The data of all researchers are described by the formula $u = Bp^\nu$ with $\nu = 0.77$–$0.82$ in the pressure range 0.2–10 MPa and with $\nu = 0.9$–$1.1$ in the range of pressures above 10 MPa.

According to our studies, strands pressed from pure crystallized HMX are incapable of burning at subatmospheric pressures. In the case of atmospheric pressure, it is difficult to ignite such strands, and they burn with further extinction. Available data of other laboratories were also obtained at pressures above the atmospheric value. For this reason, the atmospheric pressure can be considered as the low-pressure limit of pure HMX combustion. At the same time, HMX combustion at subatmospheric pressures down to 0.05 MPa was described in [15, 26].

A similar situation was observed earlier in studying combustion of ammonium dinitramide (ADN) [27]. As in the case with ADN, a possible reason of the differences in the low-pressure limit of HMX combustion is the presence of small amounts of various additives (both organic and inorganic) in the high explosive.

Our research revealed stable combustion of 10-mm strands of HMX containing 3.5% of an organic hydrocarbon phlegmatizing agent down to pressures of 0.025 MPa. It is also well known that a typical additive formed at the stage of HMX production is another cyclic nitramine, namely, cyclotrimethylenetrinitramine (RDX). It turned out that HMX containing a 5% well-distributed RDX additive burns well at least down to pressures of 0.05 MPa.

Burning of HMX doped with 5% of RDX at subatmospheric pressures is accompanied by a flame, while phlegmatized HMX burns in the flameless regime in the pressure interval 0.025–0.03 MPa, and the flame appears only at $p \geqslant 0.05$ MPa. HMX combustion in the flameless regime is accompanied by formation of a large amount of smoke, which makes the burning rate measurements more difficult.

Figure 2 shows the burning rate of HMX doped with 5% of RDX and also the data of [15] and [26] obtained in the range of low pressures. All results are seen to be grouped around the line extrapolated from the interval $p = 0.2$–$10$ MPa.

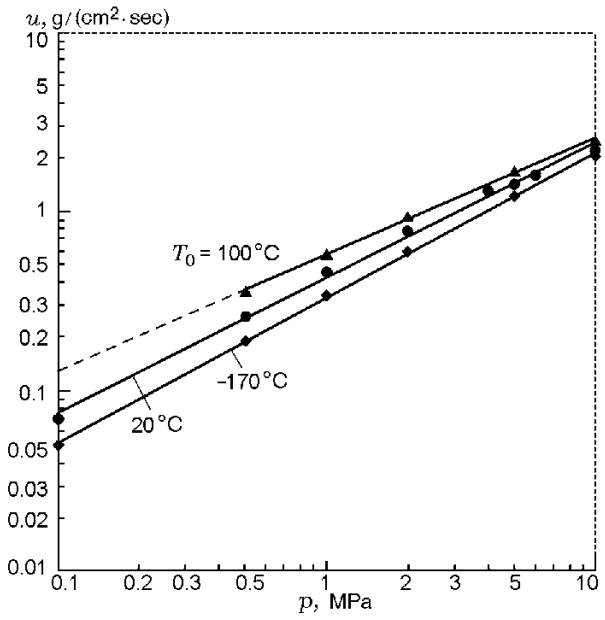


**Fig. 3.** HMX burning rate versus pressure at different initial temperatures [15].

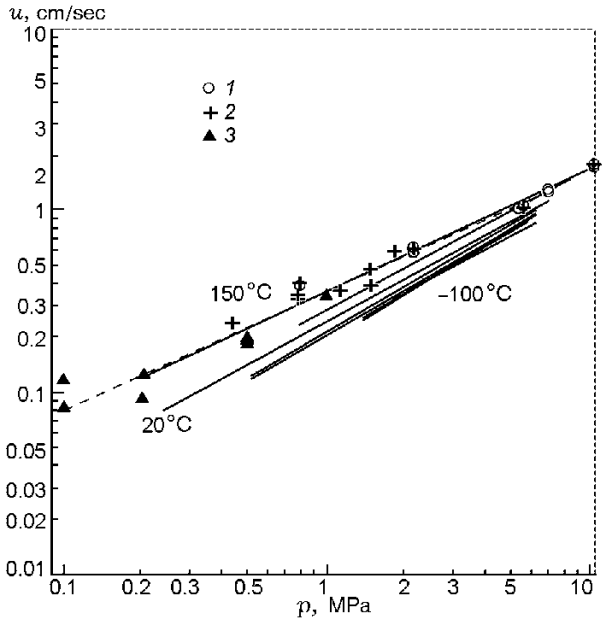


**Fig. 4.** HMX burning rate versus pressure at different initial temperatures: experimental data at $T_0 = 150°C$ obtained in [24] (1), in [2] (2), and in the present work (3); no experimental points for other temperatures are given.

## HMX Combustion at Different Initial Temperatures

The influence of the initial temperature on HMX combustion in a wide range of pressures was thoroughly studied by American scientists [2, 11, 24, 28, 29] and Russian scientists [14, 15]. Data on combustion of HMX single crystals and pressed samples at room temperature and elevated temperatures (100 and 150°C) were published in [2, 28]. Parr et al. [29] extended this research to the range of low temperatures (0, −25, −50, −75, and −100°C). All these data were summarized in Boggs' review [11].

Zenin et al. [14] and Zenin and Finjakov [15] studied combustion of 15 × 15 × 10 mm strands of pressed HMX with a density 1.70–1.77 g/cm$^3$ in the range of pressures $p$ = 0.1–10 MPa at temperatures $T_0 = 100$, 20, and −170°C. The burning rates reported in these publications are somewhat different, especially at $T_0$ = 100°C. Figure 3 shows the data of the latest experiments [15], the point at $p$ = 0.1 MPa and $T_0 = -170°C$ from [14], and also the extrapolation of the dependence $u(p)$ at $T_0$ = 100°C to atmospheric pressure. According to the data obtained, the power index in the burning law decreases from 0.81 to 0.65 with increasing initial temperature. The major part of measurements in [24] were made in the range of pressures 0.79–6.21 MPa at temperatures $T_0 = -100$, −75, −50, −25, 0, 25, 100, and 150°C. In the last case, significant changes in the burning law should be mentioned: the power index in the burning law $\nu$ in the temperature interval from $T_0 = -100°C$ to 100°C weakly decreases from 0.84 to 0.78, while its value at $T_0 = 150°C$ reaches 0.65 (Fig. 4).

It should be noted that the authors of [2, 11, 24, 28, 29] reported the values of all experimental points obtained, whereas only the mean values are given in other publications. Our data obtained at $p$ = 0.1, 0.2, 0.5, and 1 MPa and at $T_0 = 150$ and 20°C are in reasonable agreement with the data of American publications (see Fig. 4).

Figure 5 shows the HMX burning rates versus the initial temperature at $p = 0.1$ and 0.5 MPa, which were obtained by different authors. As pure HMX has the low-pressure limit around $p \approx 0.1$ MPa, Simonenko et al. [30] studied HMX combustion with addition of soot. In the present work, we consider combustion of HMX with a 5% additive of RDX, which also increases the low-pressure limit of HMX combustion. There was no information about the additives in [14, 15], but it is known that the HMX sample studied in [15] was capable of burning in vacuum. The burning rates measured by Atwood et al. [24] were extrapolated to 0.5 MPa (except for a few measured points) and to 0.1 MPa. The data of Zenin et al. [14] were supplemented with the point

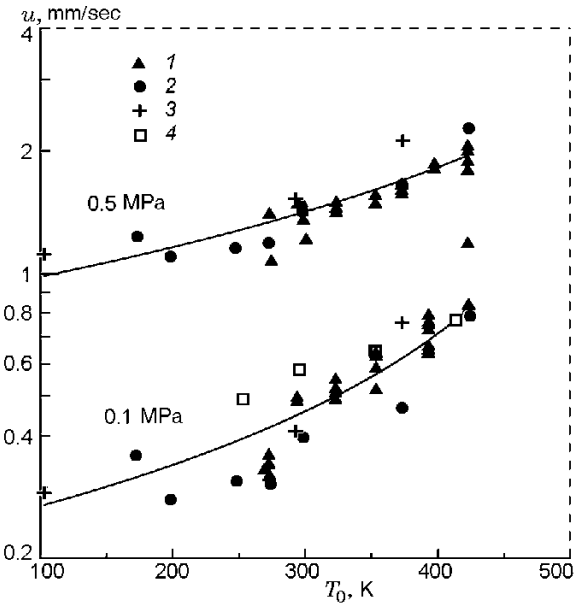


**Fig. 5.** HMX burning rate versus the initial temperature at $p = 0.1$ and 0.5 MPa: 1) strand 10 mm in diameter in a tube; 2) strand $5 \times 6$ mm, extrapolation [24]; 3) strand $15 \times 15 \times 10$ mm [15]; 4) strand 10 mm in diameter in a tube [30]; the curves are the approximations of the generalized experimental data.

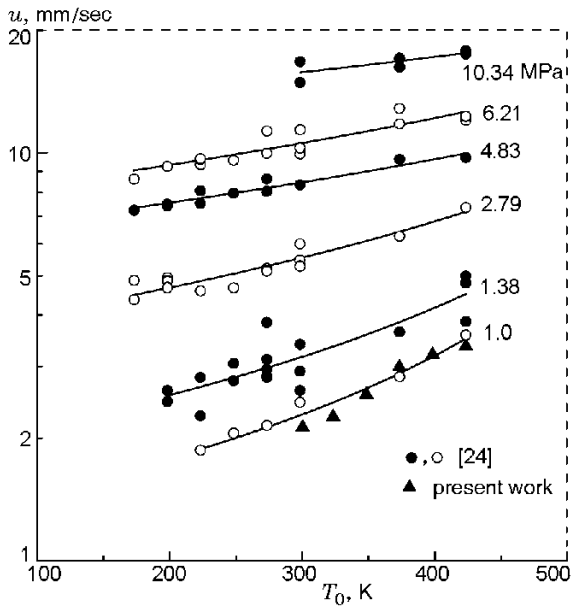


**Fig. 6.** HMX burning rate versus the initial temperature at different pressures.

at $T_0 = 100$°C obtained by extrapolation from high pressures [15].

As is seen from Fig. 5, the scatter in the values of HMX burning rates reaches 35%, which is substantially greater than the standard measurement error of 5%. Moreover, the HMX burning rates measured by different authors are also considerably different. Though the diameters of the examined samples vary from 6 to 15 mm, the difference in the burning rate cannot be attributed to the influence of the critical diameter of combustion. Apparently, the inhibition technique is rather important, as well as the presence of impurities or special additives. The correspondence between the burning rates becomes much better at elevated pressures (Fig. 6).

Figure 6 shows the HMX burning rates versus the initial temperature in the range of pressures from 1 to 10.34 MPa [24]. The figure also contains our data at $p = 1$ MPa, which agree well with the burning rates determined from the dependences $u(p)$ reported in [24].

It is seen from Fig. 5 that our experimental data, as well as the results of other authors, are adequately described by the dependence $u = A/(B - T_0)$. The same formula describes the data on $u(T_0)$ obtained in [24] in the range of pressures 0.79–10.34 MPa (see Fig. 6). All these facts testify to the leading role of condensed-phase reactions in a wide range of pressures. Knowing the HMX surface temperature at different pressures, the change in $u(T_0)$ can be described as $u = A/(T_s - T_0)$ in accordance with the c-phase model. In this case, however, only experimental points at pressures $p > 1$ MPa are adequately described, while the burning rates at lower pressures cannot be described by a dependence with a fixed surface temperature: experimental data are more sensitive to temperature variations than the c-phase model implies. Obviously, these differences are not related to thermal instability, because the dependence fails to describe points at high rather than at low temperatures. Apparently, such a drastic temperature dependence at low pressures is associated with the transition of combustion to another mode at high initial temperatures.

## Temperature Sensitivity of the HMX Burning Rate

Differentiating the dependence $\ln u(T_0)$, we can find the temperature sensitivity of the burning rate ($\beta$) as a function of the initial temperature. The temperature sensitivity of HMX at atmospheric pressure, predicted by the c-phase model, is compared with experimental data in Fig. 7. It is seen that all data have a form typical for combustion with the leading reaction in the condensed phase. The temperature sensitivity calculated on the basis of our data and the data of [14, 15] (as well as the temperature sensitivity estimated on the basis of the extrapolated data [24]) differs significantly

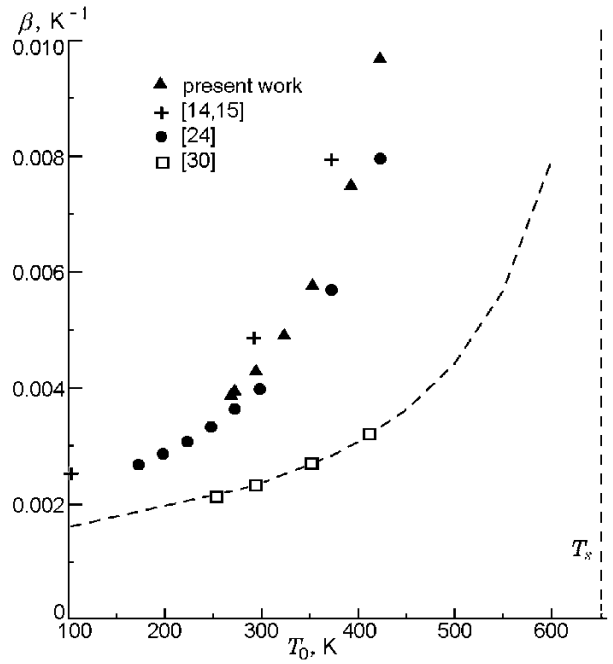


**Fig. 7.** Comparison of temperature sensitivity of HMX at atmospheric pressure, calculated by the c-phase model (curve), with experimental data (points).

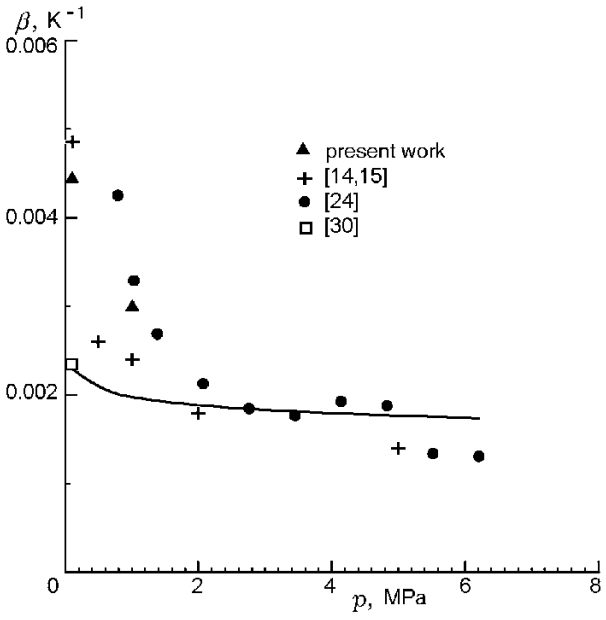


**Fig. 8.** Comparison of temperature sensitivity of HMX at different pressures, calculated by the c-phase model (curve), with experimental data (points).

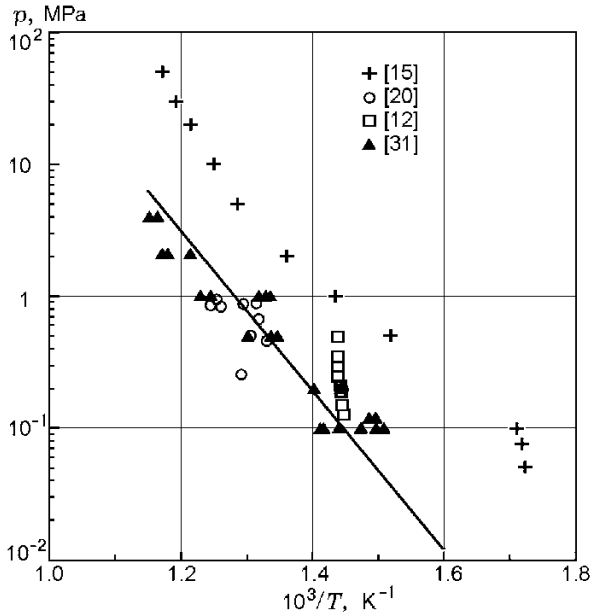


**Fig. 9.** HMX surface temperatures at different pressures.

from the theoretical curve, while the values of $\beta$ calculated on the basis of the data obtained in [30] are described by the theoretical curve. In the latter case, we can assume that it is not a random coincidence caused by a large uncertainty in determining the differential value of $\beta$. A probable reason is the effect of soot addition, which increases the heat income from the gas phase due to radiation (by changing the c-phase emissivity factor) and simultaneously prevents an anomalous increase in the melted layer thickness [31].

Experimental values of the temperature sensitivity of HMX at different pressures are compared in Fig. 8 with the dependence $\beta(p)$ calculated by the c-phase model. It is seen that the experimental values of $\beta$ at $T_0 = 20°C$ are close to the calculated dependence $\beta(p)$ at $p > 2$ MPa. At lower pressures, both our data and the data of [14, 15] exceed the calculated values. The increase in temperature sensitivity with approaching the low-pressure limit of combustion is usually associated with thermal instability due to higher heat losses. As was noted above, however, the increase in $\beta$ for HMX with decreasing pressure seems to be related to the transition of combustion to another mode at elevated initial temperatures. The fact that it is the situation at elevated initial temperatures where the increased values of $\beta$ are caused by a significant increase in the burning rate was also noted in [32].

## Thermocouple Investigations of the HMX Combustion Wave

Thermocouple investigations of the HMX combustion wave were performed by many authors; the most detailed study, however, was reported by Zenin et al.

[13–15]. In those experiments, the temperature of the burning surface was determined by a method where the thermocouple junction was pressed to the surface with the help of small loads throughout the test; it was only at high pressures ($p > 7.5$ MPa) that the surface temperature was determined as the temperature at the inflection point on the temperature profile. In our previous work [33], as well as in [20, 12], the surface temperature was determined from a noticeable inflection on the temperature profile. The dependence of the surface temperature on pressure is plotted in Fig. 9 in the coordinates $p, T^{-1}$ for presentation of vapor pressure above a boiling surface. Our experimental points, as well as the data of Lengelle et al. [20], in the range of pressures $p = 0.1$–$4$ MPa lie on a straight line corresponding to the vapor pressure above liquid HMX, which was obtained in [5, 7] on the basis of experimental data on HMX sublimation at low pressures [34]. Though the inflection on the profiles in the pressure interval from 0.1 to 0.5 MPa is clearly visible, the scatter of data is still rather significant (up to 40 K). Apparently, this was the reason that Kubota and Sakamoto [12] declared that the HMX surface temperature is independent of pressure, which is physically meaningless.

The calculations show that the size of zones in the HMX flame at $p > 1$ MPa becomes comparable with the thermocouple size, which is a natural restriction for this method. Nevertheless, surface temperatures up to 50 MPa were reported in [14, 15].

As is seen from Fig. 9, the surface temperature determined by the inflection on the temperature profile is much higher than the temperature determined by the method with small loads. It should be noted that the HMX surface is covered with a melted layer, and the researcher cannot be sure than the pressed thermocouple is located exactly on the boiling surface rather than is immersed into the melt.

A phenomenon of flameless combustion was observed in studying phlegmatized HMX combustion. In such a regime, it is usually easier to measure the surface temperature with the help of thermocouples. In addition, the measurement accuracy is improved by expanding the range of measurements to subatmospheric pressures. For this reason, we studied the temperature distribution in the combustion wave of phlegmatized HMX at $p = 0.025$–$0.1$ MPa and HMX doped with 5% of RDX at $p = 0.05$–$0.1$ MPa.

Figures 10 and 11 show the temperature profiles in the combustion wave of phlegmatized HMX. The flameless regime of HMX combustion is observed at $p = 0.025$–$0.03$ MPa, while an unstable flame appears at a considerable distance $x$ from the surface at $p = 0.04$–$0.05$ MPa. With increasing pressure, the flame

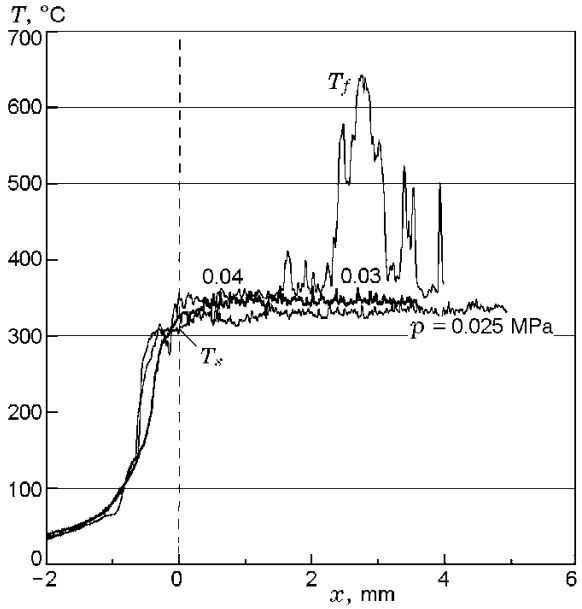


**Fig. 10.** Temperature profiles in the combustion wave of phlegmatized HMX at $p = 0.025$, 0.03, and 0.04 MPa.

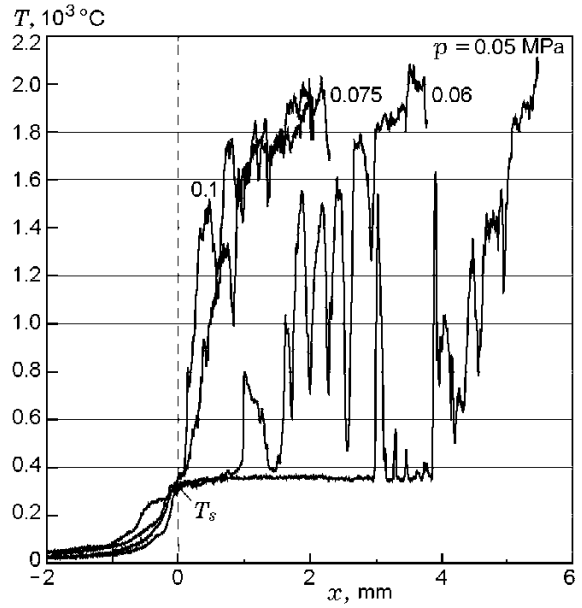


**Fig. 11.** Temperature profiles in the combustion wave of phlegmatized HMX at $p = 0.05$, 0.075, and 0.1 MPa.

becomes more stable; the distance between the flame and the surface becomes smaller and reaches ≈1 mm at atmospheric pressure. The dark zone between the flame and the surface is clearly seen in video records made at low pressures. The lower edge of the visible flame is not flat and oscillates, apparently, under the action of lo-

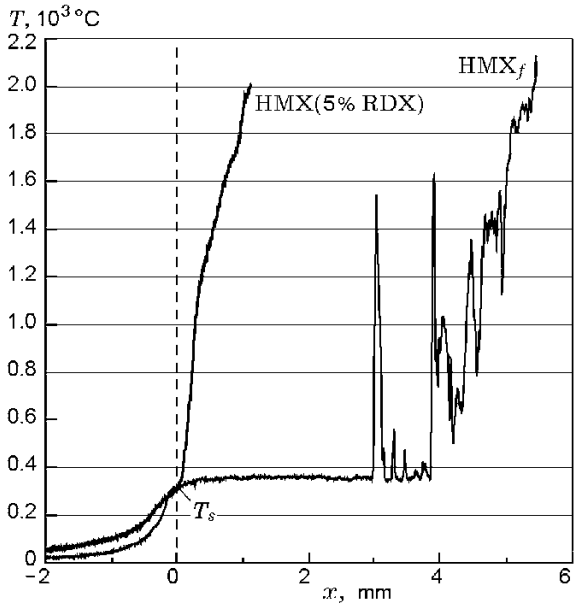


**Fig. 12.** Temperature distributions in the combustion wave of phlegmatized HMX and HMX doped with 5% of RDX at $p = 0.05$ MPa.

cal gas flows emanating from the burning surface, while the latter permanently changes its relief. The width of the dark zone (the distance between the surface and the lower edge of the visible flame) displays arbitrary changes with time (above a given surface point) and is not identical over the surface. A complicated geometric shape of the visible flame during HMX combustion at low pressures was previously observed in [12]. Zenin and Finjakov [15] also noted that the temperature field in the gas phase was nonuniform, which was attributed to gas bubbles exploding on the surface.

The oscillating lower edge of the flame can "lick" the thermocouple several times before the latter finally enters the visible flame zone. The thermocouple "licked" by the flame registers a temperature spike and then again registers the temperature of the dark zone. The flame proper seems to consist of local spots as well, because the thermocouple located completely in the flame zone still continues to register strong spikes of temperature. A comparison of video records with temperature profiles shows that the temperature is practically constant over the entire dark zone.

As was already noted, a mixture of HMX with 5% of RDX in 10-mm strands starts to burn at $p = 0.05$ MPa with an immediately formed high-temperature flame. Judging by the video records, we can see that combustion of HMX doped with 5% of RDX looks similar to combustion of phlegmatized HMX, but the dark zone is substantially narrower, and the scale of "roughness elements" on the surface relief (similar to the surface of a boiling liquid) is noticeably smaller. By comparing the temperature profiles of phlegmatized HMX and HMX doped with 5% of RDX (Fig. 12), we can mention similar values of the surface temperature and burning temperature, but much earlier formation of the gas flame and the absence of flame oscillations in the case of combustion of HMX doped with 5% of RDX.

Let us consider the promoting effect of additives on HMX combustion at subatmospheric pressures. Sinditskii et al. [27] explained a similar effect of paraffin in ADN combustion by suppression of the development of large-scale oscillations on the liquid surface, resulting in shedding of large drops by the outgoing gases and in destruction of the reactive layer. Apparently, non-polar paraffin added to a polar melt reduces the surface tension. Addition of a phlegmatizing agent to HMX seems to produce the same effect.

The role of RDX is different. RDX is a less stable and more volatile substance than HMX; hence, RDX rapidly decomposes and evaporates in the HMX melt. Nevertheless, stable combustion of the mixture at low pressures cannot be explained only by the influence of additional heat release in the condensed phase: phlegmatized HMX containing 3.5% of an inert additive is capable of burning even at lower pressures. Apparently, the role of the RDX additive, as in the case of addition of a phlegmatizing agent, has a physical nature: addition of a less stable substance prevents large-scale dispersion, for instance, owing to a uniform distribution of bubbles with gaseous products of RDX decomposition and evaporation over the melt.

A comparison of the temperature profiles of phlegmatized HMX and HMX doped with 5% of RDX shows that the phlegmatizing agent plays a double role: on one hand, it prevents large-scale dispersion; on the other hand, evaporation of a comparatively inert hydrocarbon into a gaseous mixture of HMX decomposition and evaporation products inhibits the ignition of this mixture, resulting in the emergence of an extended dark zone.

The presence of a significant plateau on the temperature profiles of phlegmatized HMX facilitates determining the surface temperature and reduces the scatter of results to 7–10°C. In the case with HMX doped with 5% of RDX, there are practically no such extended plateaus, and the surface temperature was determined as the temperature at the inflection point on the temperature profile. The values obtained are close to the surface temperature of phlegmatized HMX. The surface temperature of phlegmatized HMX at atmospheric pressure was $374 \pm 7$°C (based on four profiles). A similar surface temperature equal to 377°C was obtained in [35] in the case of laser-induced ignition of HMX.

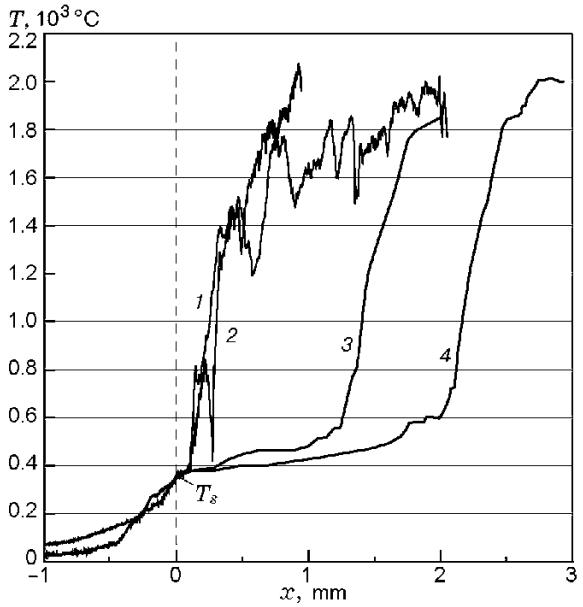


**Fig. 13.** Comparison of the temperature distributions in the wave of self-sustained combustion of phlegmatized HMX (1) and pure HMX (2) with the temperature profiles of laser-driven HMX combustion with 35 (3) and 60 W/cm$^2$ (4) at $p$ = 0.1 MPa [36].

It turned out, however, that surface temperatures determined in the present work during HMX combustion at subatmospheric pressures do not agree with out previous data [33] in the pressure range from 0.1 to 1 MPa. The difference between the mean surface temperatures at the matching point at atmospheric pressure was ≈40°C: it looks as if the surface temperature at lower pressures is shifted in parallel to the range of lower temperatures.

A repeated analysis of the temperature profiles obtained previously shows that most of them, in addition to a sharp inflection (at the moment when the thermocouple enters the high-temperature zone), contain a typical point close to the surface temperature of phlegmatized HMX, which lies ahead of the sharp inflection on the profile (Fig. 13). At atmospheric pressure, this point in most cases is located at a distance of ≈150 $\mu$m from the sharp inflection on the profile and corresponds to a temperature of 380±13°C (based on eight profiles).

In the range of subatmospheric pressures, the gas flame above the surface of phlegmatized HMX occurs in the induction regime (see Figs. 10 and 11). We can assume that the condensed-phase reactions continue to play the leading role at elevated pressures and that the sharp inflection on the profiles, which was considered as the temperature surface, is actually the temperature of ignition of the gas flame. This assumption is supported by a comparison of the temperature distributions in the wave of self-sustained combustion of HMX with the temperature profiles of laser-driven HMX combustion [36] at atmospheric pressure (see Fig. 13). As is seen from Fig. 13, an increase in the laser radiation density from 35 to 60 W/cm$^2$ increases the ignition temperature of the gas flame (drastic increase in temperature on the profiles) from 560 to 600°C, whereas the surface temperature remains almost constant: 357–362°C. Using the experimental data on the surface temperature, burning rate, composition and concentrations of the gas-phase species above the HMX surface, and the set of elementary reactions in nitramine flames [37], Kudva and Litzinger [36] calculated the temperature profiles in the gas phase with the use of the CHEMKIN code. Their calculations revealed reasonable agreement with experimental profiles, which confirms the possibility of gas-flame ignition in the induction mode at certain rates of the process in the condensed phase.

As was already noted, the power index in the dependence $u(p)$ becomes substantially lower at $T_0 > 100$°C. The reason is a more drastic increase in the burning rate at elevated initial temperatures in the pressure interval $p < 1$ MPa than at higher pressures. A similar behavior of the powder N should be noted: the dependence $u(T_0)$ at $p = 1$ and 2 MPa is significantly steeper than that at $p = 5$ MPa [38].

To elucidate the reasons for this behavior, we studied the temperature distribution in the combustion wave of HMX doped with 5% of RDX at $T_0 = 120$ and 150°C. Combustion at these temperatures is accompanied by gas-flame oscillations. The thermocouple data display drastic oscillations of temperature at instants when the thermocouple passes through the gas flame; in some cases (three out of seven cases at $T_0 = 120$°C and one out of three cases at $T_0 = 150$°C), regular oscillations with a frequency of 6.5–7 Hz and increasing amplitude are observed (Fig. 14). As the thermocouple moves in the flame, the envelope of the temperature peaks increases and approaches the maximum value, which testifies to the formation of a typical flame structure with $T_f$ = 2000–2050°C (the losses due to radiation are ignored) at each peak. As is seen for the profile in Fig. 14, the temperature decreases to $T_s$ after the peak in the gas phase. The surface temperature at $T_0 = 120$°C is 380 ± 3°C (based on seven profiles), which shows that the surface temperature remains unchanged with increasing initial temperature.

Such regular oscillations were observed only in the case of strand combustion in Plexiglas tubes, and there were no regular oscillations at the initial moment of combustion and immediately before combustion failure. An analysis of video records shows that similar flame

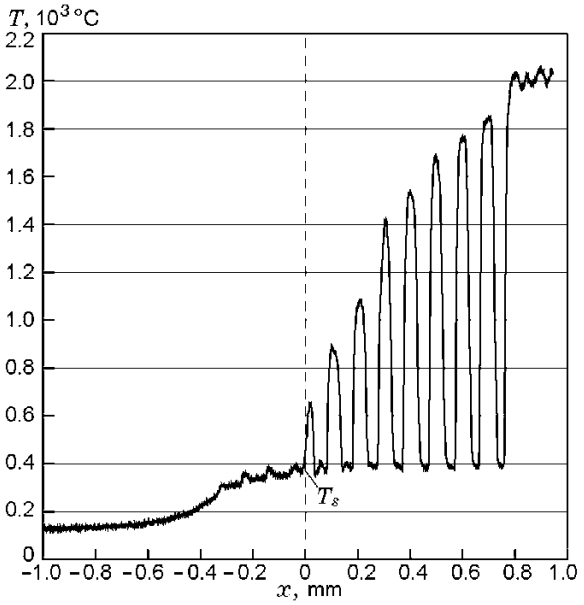


**Fig. 14.** Temperature profile in the combustion wave of HMX doped with 5% of RDX at atmospheric pressure and initial temperature of 120°C.

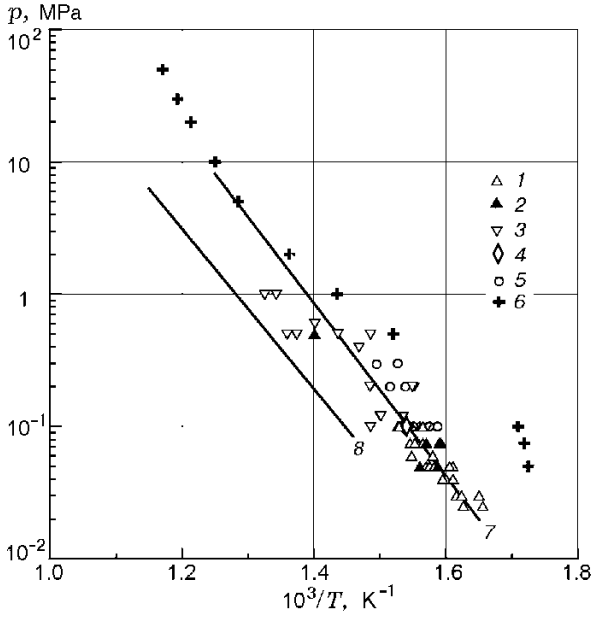


**Fig. 15.** HMX surface temperature at different pressures: phlegmatized HMX (1), HMX doped with 5% of RDX (2), pure HMX (3), data [35] (4), data [39] (5), and data [15] (6); the curves show the vapor pressure above liquid HMX obtained in the present work (curve 7) and in [5] (curve 8).

oscillations are sometimes observed in combustion of HMX doped with 5% of RDX in tubes at room temperature.

All results on the surface temperature of phlegmatized HMX and HMX doped with 5% of RDX are summarized in Fig. 15 in the coordinates $p(T^{-1})$. The figure also shows the refined HMX surface temperatures based on the previous [33] thermocouple measurements, the data of [15], and the surface temperatures obtained in experiments on laser-driven HMX ignition [35] and combustion [39].

Figure 15 also shows the vapor pressure above the HMX melt: the lower curve was plotted in [5], and the upper curve was obtained in the present work. The vapor pressure above solid HMX was measured in experiments in [34, 40, 41], which showed that the heat of HMX sublimation is 38.5–38.7 kcal/mole. Prior to melting, HMX experiences a solid-phase transition from the $\beta$ to the $\delta$ modification; the heat of this transition is estimated as 2.35 kcal/mole [42]. As HMX starts to decompose intensely during its melting, it is impossible to measure the melting heat directly; hence, it is determined by indirect methods. Maksimov [43] determined the HMX melting heat (16.7 kcal/mole) from the melting diagram of the RDX–HMX system. In the case of dissolution of a solid substance in a solvent that does not interact with the dissolved substance, the dissolution heat can be considered as the melting heat. Korobko et al. [44] showed that the heats of HMX dissolution in acetone, butyl acetate, and aniline are close to each other and amount to ≈6.3 kcal/mole, which is substantially lower than the data obtained in [43]. American researchers also use a lower melting heat of HMX: 8.34 kcal/mole [32]. Based on the dissolution heat, the heat of the phase transition, and sublimation heat, we assumed the evaporation heat to be 28 kcal/mole in the present work. Based on this value and numerous consistent data on the surface temperature at atmospheric pressure (377–380°C), the following dependence of the surface temperature on pressure was derived:

$$\ln p = -14{,}092/T + 21.72.$$

As is seen from Fig. 15, this dependence offers an adequate description of almost all experimental data. The results of [15] approach this dependence only at high pressures; the difference at low pressures is rather large.

## Heat of the Reaction in the Condensed Phase

To elucidate the combustion mechanism, it is important to know the thermal effect of the reaction ($Q$) in the condensed phase. Many researchers who

TABLE 1

Heat Effect in the Condensed Phase ($Q_c$) and Heat Effect of the Decomposition Reaction in the Condensed Phase ($Q$)

| $p$, MPa | $Q_c$, cal/g | $Q$, cal/g | Reference |
|---|---|---|---|
| 0.1–0.5 | 71.7 | — | [12] |
| 0.5–10 | From 60 to 100 | — | [20] |
| 0.1–10 | 95.6 | — | [8] |
| 0.05–10 | From −92 to 192 | — | [15] |
| 2–5 | From −78.8 to −72.8* | 202.7 | [4] |
| 2–5 | — | 171.4 | [3] |
| 0.1 | 142.8* | 268.1* | [49] |
| 0.1–10 | From 65.2 to 19.8* | 360 | [5] |
| 0.05–56 | — | 357–382 | [7] |
| 0.1 | — | 331.5 | [45] |
| 0.1 | — | 331.3 | [46] |
| 0.03 | 154 | 192.5 | Present work |

**Note.** The authors' calculations on the basis of given data are marked by an asterisk; the value $Q = 331.3$ cal/g corresponds to the mixture with 5% of a polyurethane binder.

studied and modeled HMX combustion used versatile value of the heat effect in the condensed phase $Q_c = \eta Q - (1-\eta)Q_{\text{ev}}$. As the depth of HMX decomposition in the c-phase ($\eta$) is not known, this heat effect consists of the contributions of heat release due to the chemical reaction $\eta Q$ and the heat spent on evaporation of the non-decomposed substance $(1-\eta)Q_{\text{ev}}$. Based on thermocouple measurements, it was concluded that the processes in the condensed phase are exothermal: the heat effect is either constant (71.2 cal/g [12] and 95.6 cal/g [8]) or slightly increases with pressure from 60 to 100 cal/g [20] (Table 1). Zenin and Finjakov [15] obtained $Q_c = -92$–192 cal/g with pressure variations in the range 0.05–10 MPa.

The heat effect of the decomposition reaction in the condensed phase can be measured directly by means of differential scanning calorimetry, but its value can be underestimated owing to the endothermal process of evaporation proceeding simultaneously with exothermal decomposition. Lee et al. [45] measured the heat effect of decomposition at different heating rates; the maximum value was 331.5 cal/g. Singh et al. [46] obtained a similar value of 331.3 cal/g in studying combustion of HMX doped with 5% of a polyurethane binder.

The heat effect of the decomposition reaction in the melt can also be found by determining the content of decomposition products. The thus-obtained heat effect varies from 171.4 [3] and 202.7 cal/g [4] in early works to 268.1 cal/g in the recent work [47].

Finally, the heat effect for nitrocompounds is usually estimated on the basis of the primary flame temperature under the assumption that secondary reactions in the condensed phase produce the same products as the reactions in the primary flame. The heat effect equal to 360 cal/g [5] and the heat effect of 357–382 cal/g slightly varying with time [7] seem to be determined for the temperature of the primary flame of HMX combustion equal to 1320 K.

As we managed to obtain conditions of flameless combustion, we could estimate the heat effect of the decomposition reaction by measuring the amount of nonreacted HMX after combustion. In the c-phase model of combustion, the depth of decomposition of the energetic material in the condensed phase is determined by the ratio of heat needed for heating of the substance to the surface temperature with allowance for the amount of heat spent on melting and (or) phase transitions ($L_m$) to the heat effect of the decomposition reaction:

$$\eta = \frac{c_p(T_s - T_0) + L_m}{Q}. \tag{1}$$

The remaining non-decomposed substance is dispersed to the gas phase by the outgoing gaseous products of decomposition and continues to decompose (evaporate) there with no significant influence on the burning rate.

After combustion of the HMX strand in the flameless regime at $p = 0.03$ MPa, there remain 20% of the solid residue, which consists of HMX, as is shown by IR spectroscopy. Knowing $T_s$ and the temperature dependence of the HMX specific heat in the solid [48] and liquid [32] states, we can estimate the reaction heat as $Q = 192.5$ cal/g. This value is slightly underestimated, because some of the small HMX particles could have escaped collection. The value obtained is substantially lower than the amount of heat released in the primary flame. Adiabatic calculations show, however, that a change in pressure from 10 to 0.03 MPa leads to a decrease in the primary flame temperature by 300–400°C, which is fairly comparable with the change in the reaction heat from 360 to 190 cal/g. Based on this result and on the data of [5, 7, 45–47], we further assumed that the decomposition-reaction heat $Q$ is a variable quantity and described it by the expression $Q$ [cal/g] $= 320 + 20 \ln p$ in the pressure range $p = 0.03$–10 MPa.

### Kinetics of Heat Release in the Condensed Phase

Thermocouple measurements showed that the high-temperature flame occurs in the induction regime, at least up to pressures of 1 MPa, and does not affect the burning rate (if the radiative heat flux from the gas phase is ignored). The curve of the HMX burning rate as a function of pressure has no inflections up to 10 MPa; therefore, it is little probable that the combustion mechanism experiences any drastic changes in this range of pressures. To answer the question about the contribution of condensed-phase reactions at high pressures, however, one should know the kinetics of heat release in this phase.

Based on the experimental dependence of the surface temperature on pressure and experimental values of the HMX burning rate, we calculated the heat-release rate constants in the c-phase, using the expression for the burning rate from the c-phase model of combustion [22]:

$$m = \left[\frac{2\lambda\rho Q}{c_p^2(T_s - T_0 + L_m/c_p)^2}\left(\frac{RT_s^2}{E}\right) \times A\exp\left(-\frac{E}{RT_s}\right)\right]^{1/2}. \quad (2)$$

In these calculations, we took into account the heat spent on the phase transition and melting ($L_m$), the changes in the specific heat $c_p$ and thermal conductivity $\lambda$ of the condensed phase [32], and also the varying heat of the decomposition reaction $Q$.

The results obtained ($k = 6.0 \cdot 10^{18} \times \exp(-46{,}575/RT)$, $\sec^{-1}$) are plotted in Fig. 16 together with the data on HMX decomposition in the liquid phase reported in various publications. As is seen from the figure, the rate constants of heat release in the condensed phase are close to the rate constants of HMX decomposition obtained by other methods at lower temperatures, which testifies that the rate of heat release in the c-phase during HMX combustion is determined by the kinetics of HMX decomposition.

In Table 2, we compare the heat needed for heating, phase transition, and melting,

$$Q_{\text{need}} = c_p(T_s - T_0) + L_m, \quad (3)$$

with the heat generated in the condensed phase $Q_s = \eta Q$, where the decomposition depth is estimated by the formula

$$\eta = \frac{2\lambda\rho RT_s^2 A\exp(-E/RT_s)}{c_p m^2 E(T_s - T_0 + L_m/c_p)}, \quad (4)$$

which takes into account the rate constant of HMX decomposition at the surface temperature and the residence time of the substance in the reaction zone, determined by the burning rate. As is seen from Table 2, the needed and actually released amounts of heat are in good agreement. This agreement testifies that the heat release in the condensed phase covers the heat expenses for the phase transition, melting, and heating of the substance to the surface temperature, at least, up to 10 MPa.

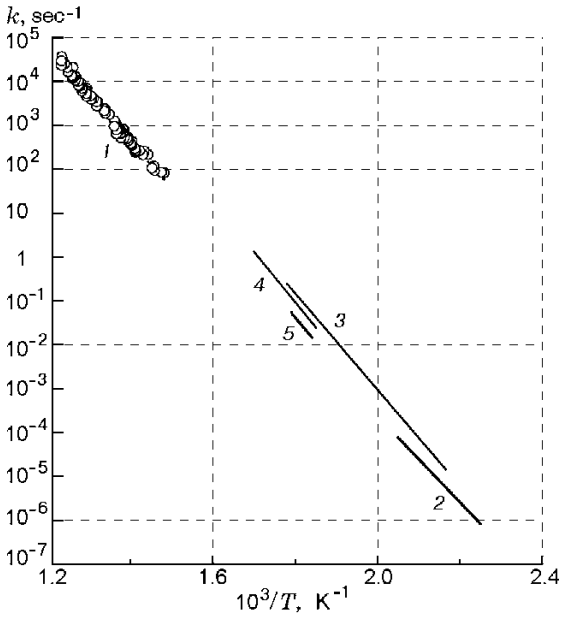


**Fig. 16.** Comparison of the kinetic parameters of heat release in the condensed phase of HMX (points 1) and HMX decomposition in the nitrobenzene solution (curve 2 [49]), acetone (curve 3 [50]), and melt (curves 4 [51] and 5 [52]).

TABLE 2

Comparison of Heat Needed for Heating to the Surface Temperature ($Q_{\text{need}}$) with the Amount of Heat Released in the Condensed Phase ($Q_s$)

| $p$, MPa | $\eta$, % | $Q_{\text{need}}$, cal/g | $Q_s$, cal/g |
|---|---|---|---|
| 0.1 | 71 | 170 | 194 |
| 0.5 | 70 | 195 | 214 |
| 1 | 69 | 207 | 222 |
| 2 | 68 | 220 | 228 |
| 5 | 67 | 240 | 235 |
| 10 | 65 | 256 | 238 |

### HMX Combustion Mechanism

An analysis of available data and the results obtained allow us to propose the following mechanism of HMX combustion. In a wide range of pressures and

initial temperatures, the HMX combustion process is governed by condensed-phase reactions with the kinetic parameters corresponding to the initial stage of HMX decomposition. The heat release in the condensed phase completely compensates for the expenses of heat spent on heating the substance to the surface temperature; the heat incoming from the gas phase is spent only on evaporation of the non-decomposed portion of HMX and does not exert any influence on the burning rate.

It should be noted that Ward et al. [8] proposed a mechanism of HMX combustion based on the exothermal c-phase reaction and heat income from the gas phase. To describe the processes in the condensed phase, Ward et al. used Lengelle's model [53] with allowance for the heat income from the gas phase and noted that this model was previously proposed by Merzhanov and Dubovitskii [54]. According to [8], the burning rate in the range of initial temperatures from $-75$ to 150°C and in a wide range of pressures is described by this model, if the activation energy of gas-phase processes is assumed to be close to zero. Obviously, this means that the gas phase is insensitive to changes in the burning temperature.

Experimental and calculated dependences of the burning rate on pressure at different initial temperatures and on initial temperature at different pressures are compared in Figs. 17 and 18. The calculated values are in good agreement with the experimental results in the range of pressures $p = 1$–10 MPa and initial temperatures $T_0 = -170$–100°C. Deviations of the experimental data from the calculated curves are observed at high initial temperatures ($T_0 > 100$°C) and low pressures ($p < 1$ MPa).

Let us consider possible reasons for that. Washburn and Beckstead [32] attributed high burning rates at elevated initial temperatures and low pressures to an increased thickness of the melt layer under these conditions, which yields a longer residence time of the substance in the liquid phase and, correspondingly, a greater degree of decomposition. If the temperature in the melt, however, is assumed to follow the Michelson distribution and the decomposition reaction proceeds in a narrow reactive layer near the surface, then shorter residence times can be expected to correspond to higher burning rates. The higher the initial temperature, the smaller heat expenses on heating the substance to the surface temperature and the smaller the depth of decomposition in the condensed phase. The c-phase model of combustion predicts that it is the lower expenses on substance heating to the surface temperature that are responsible for the increase in the burning rate with increasing initial temperature. Our thermocouple investigations show that the surface temperature does not

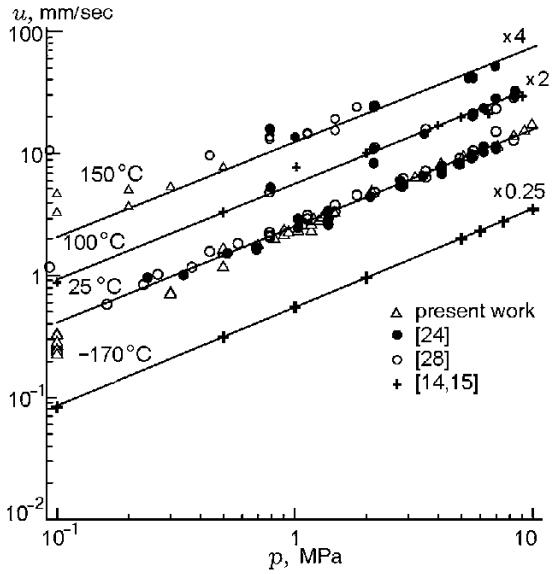


**Fig. 17.** Comparison of experimental values of the HMX burning rate (points) with results calculated by the c-phase model (curves) at different initial temperatures.

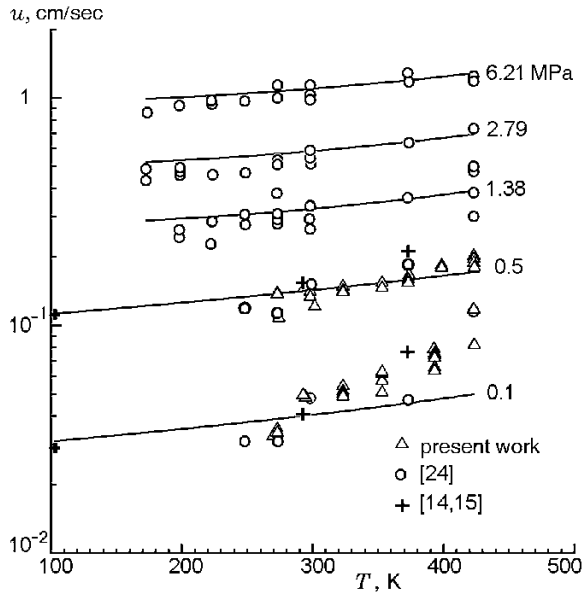


**Fig. 18.** Comparison of experimental values of the HMX burning rate (points) with results calculated by the c-phase model at different pressures.

change with increasing initial temperature; hence, the rate of heat release in the condensed phase does not change either. The increase in the initial temperature, however, affects the rate of heat release in the gas phase: first, via the increase in the burning rate and, second, via the increase in reagent concentrations in the flame,

because the degree of decomposition in the condensed phase becomes lower. Thus, at a certain initial temperature, the heat flux from the gas phase can reach the burning surface and affect the burning rate.

Another specific feature of HMX combustion is related to the change in the heat balance, namely, the change in the value of $\nu$ at high pressures. As the pressure increases, the boiling temperature may reach its critical value; in this case, the evaporation heat decreases to zero. Possibly, a more drastic increase in the burning rate at $p > 13$–15 MPa is due to a greater contribution of heat from the gas phase to the total heat balance on the surface, if the growth of the burning rate is not related to the contribution of convective heating, as it was assumed in [14].

An analysis of video images shows that, in the case of HMX combustion at atmospheric pressure, the dark zone persists at elevated temperatures as well, which excludes conductive heat income from the gas phase. Simultaneously, the humps and valleys on the boiling surface become noticeably greater with increasing initial temperature. Taking into account that the width of the melted layer increases with increasing initial temperature, as is evidenced by thermocouple measurements (our results and those reported in [15]), we can assume the reasons for elevated burning rates to be the increase in the combustion surface area owing to more vigorous boiling at elevated initial temperatures and the deviation from the laminar burning regime.

As is seen from Fig. 17, the deviation of the experimental data from the calculated curve ceases at $p > 1$ MPa. It is well known that the width of all zones in the combustion wave decreases with increasing pressure, which is expected to prevent the development of oscillations in the liquid phase. In addition, the increase in pressure can reduce oscillations owing to increasing density of the gases. Apparently, surface distortions become insignificant as the pressure increases above 1 MPa, despite the high initial temperatures.

As our thermocouple measurements show, combustion of both pure HMX and HMX with additives at reduced pressures is accompanied by flame-temperature oscillations, which may transform to regular oscillations of the gas flame in the case of strand combustion in a tube (6.5–7 Hz at $T_0 = 120$°C). The thermocouple measurements in [15] also revealed temperature oscillations in the HMX flame at $p = 0.05$–0.3 MPa, which was attributed to large bubbles bursting on the surface, thus, being responsible for a nonuniform temperature field. The self-oscillatory regime of combustion of HMX doped with 0.5% of lamp black (in pressed strands 8–16 mm in diameter in quartz tubes) at atmospheric pressure was observed in [55]. Measurements by a thrust sensor displayed the presence of comparatively regular oscillations of the thrust force with a frequency of 4.5–6 Hz at $T_0 = 20$°C and 8–10 Hz at $T_0 = 140$°C. Oscillations of the concentrations of gas-phase components, surface temperature, and burning rate with a frequency of $4 \pm 0.2$ Hz were also found in combustion of HMX strands 6.4 mm in diameter under the action of laser radiation with a power density of 30 W/cm$^2$ at atmospheric pressure [56]. Tang et al. [56] associated these oscillations with the presence of two competing chemical processes in the condensed phase. Our research shows, however, that the oscillations of the concentrations of gas-phase species are undoubtedly related to the presence or absence of the gas flame. Regular bursts of the gas flame may also be responsible for the oscillations of the burning rate and thrust.

The present investigations show that the heat flux from the gas phase onto the surface is spent only on evaporation of non-decomposed HMX in a wide range of pressures at a standard temperature. Combustion of the gas flame at low pressures involves oscillations because different points on the surface have different compositions of combustion products: the bursting bubbles contain mainly gaseous products of decomposition, HMX evaporates from the surface, and melt droplets are shed from the surface. In the case of HMX combustion in tubes, these random oscillations acquire a regular character, apparently, by the mechanism of evolution of low-frequency instability of combustion in a semi-closed volume [57]. Because of pressure oscillations, the burning rate of the gas phase at the instant with the maximum pressure exceeds the rate of the income of fresh portions of the substance from the condensed phase. The situation is aggravated by the fact that the heat released in the gas phase is spent mainly on heating of the gas phase and on evaporation of only a small fraction of HMX. As the gas phase cannot ensure a needed rate of HMX evaporation (because of the inertia of the condensed phase and because of the absence of a necessary amount of heat), the ignition after rapid burnout of the gas mixture occurs only when the reaction in the condensed phase recovers a necessary concentration of reagents in the gas and when an appropriate induction period passes. The increase in the initial temperature further enhances the rates of chemical reactions in the gas, which results in more frequent flashes in the flame, but the energy released is still spend mainly on the inherent needs of the gas phase. If external energy is supplied (the laser power density is increased up to 100 W/cm$^2$), the oscillations vanish [56], which may be explained by the fact that the heat income from the gas phase becomes capable of providing a sufficient rate of gasification of the condensed phase.

## CONCLUSIONS

The structure of the HMX flame with different additives was studied with the help of thin tungsten–rhenium thermocouples in the pressure range from 0.025 to 1 MPa. The reason for HMX combustion at reduced pressures is found: the presence of an additive (for instance, a phlegmatizing agent or RDX). An apparent role of the additive is suppression of large-scale dispersion. A flameless regime of combustion of phlegmatized HMX at subatmospheric pressure is found. A comparison of the HMX profiles for different combustion regimes allows us to assume that the gas flame ignites in the induction mode, at least, at pressures up to 1 MPa; hence, the point of the drastic increase in temperature in the combustion wave in this range of pressures is not consistent with the surface temperature. The heat effect in the condensed phase is demonstrated to be sufficient for heating the substance to the surface temperatures at pressures up to $p = 10$ MPa.

Results of the present work and available data on HMX combustion at different initial temperatures are analyzed. The temperature sensitivity of HMX is demonstrated to increase with increasing initial temperature at pressures from 0.1 to 10 MPa, which is typical for combustion with the leading reaction in the condensed phase. The burning rate calculated by the c-phase model with allowance for experimentally determined surface temperatures and HMX decomposition kinetics deviates from experimental data at pressures below 1 MPa and initial temperatures above 100°C, and also at pressures above 13–15 MPa, which is associated with a greater contribution of heat from the gas phase to the total heat balance on the surface.

The experimental values of temperature sensitivity in the pressure range from 0.1 to 1 MPa exceed the values predicted by the c-phase model, which is caused by the transition to another combustion mode at high initial temperatures rather than by thermal instability of combustion.

An analysis of available data and the results obtained in the present work allowed us to propose a mechanism of HMX combustion, based on the leading role of the reaction of HMX decomposition in the melt at the surface temperature. In the pressure interval from 1 to 10 MPa and initial temperatures from −170 to 100°C, the heat flux from the gas phase onto the surface is spent only on evaporation of non-decomposed HMX and does not affect the burning rate.

The oscillatory regime of HMX combustion, which was registered in thermocouple investigations at atmospheric pressure, is assumed to occur, on one hand, owing to the emergence of resonance phenomena during combustion of an inhomogeneous gas mixture in a tube and, on the other hand, owing to disagreement between the rate of the chemical reaction in the gas phase at the resonance instant and its energy capacity, which does not allow a needed rate of HMX gasification to be ensured.

Participation of students A. S. Efremov and A. V. Kuz'mina is acknowledged.

This work was supported by the Russian Foundation for Basic Research (Grant No. 09-03-00624-a).

## REFERENCES

1. M. W. Beckstead and K. P. McCarty, "Calculated combustion characteristics of nitramine monopropellants," in: *13th JANNAF Combustion Meeting* (1976), Vol. 1, pp. 57–68.
2. C. F. Price, T. L. Boggs, and R. L. Derr, "The steady-state combustion behavior of ammonium perchlorate and HMX," AIAA Paper No. 79-0164 (1979).
3. M. Ben-Reuven and L. Caveny, "Nitramine flame chemistry and deflagration interpreted in terms of flame model," AIAA Paper No. 79-1133 (1979).
4. N. Cohen, G. Lo, and J. Crowley, "Model and chemistry of HMX combustion," *AIAA J.*, **23**, No. 2, 276–282 (1985).
5. T. Mitani and F. A. Williams, "A model for the deflagration of nitramines," in: *Proc. 21st Symp. (Int.) on Combustion*, Combustion Institute (1986), pp. 1965–1974.
6. M. W. Beckstead, "Modeling AN, AP, HMX, and double base monopropellants," in: *26th JANNAF Combustion Meeting*, CPIA Publ. No. 529, Vol. 4 (1989), pp. 255–268.
7. S. C. Li, F. A. Williams, and S. B. Margolis, "Effects of two-phase flow in a model for nitramine deflagration," *Combust. Flame*, **80**, 329–349 (1990).
8. M. J. Ward, S. F. Son, and M. Q. Brewster, "Steady deflagration of HMX with simple kinetics: A gas phase chain reaction model," *Combust. Flame*, **114**, Nos. 3–4, 556–568 (1998).
9. J. E. Davidson and M. W. Beckstead, "A three-phase model of HMX combustion," in: *26th Symp. (Int.) on Combustion*, The Combustion Institute (1996), pp. 1989–1996.
10. K. Prasad, R. A. Yetter, and M. D. Smooke, "An eigenvalue method for computing the burning rates of RDX propellants," *Combust. Sci. Technol.*, **124**, 35–82 (1997).
11. T. L. Boggs, "The thermal behavior of cyclotrimethylenetrinitramine (RDX) and cyclotetramethylenetetranitramine (HMX)," in: K. K. Kuo and M. Summerfield (eds.), *Progress in Astronautics and*

*Aeronautics*, Vol. 90: *Fundamentals of Solid-Propellant Combustion*, Academic Press, New York (1984), pp. 121–175.
12. N. Kubota and S. Sakamoto, "Combustion mechanism of HMX," *Propell., Explos., Pyrothechnics*, **14**, No. 1, 6–11 (1989).
13. A. Zenin, "HMX and RDX: Combustion mechanism and influence on modern double-base propellant combustion," *J. Propuls. Power*, **11**, No. 4, 752–758 (1995).
14. A. A. Zenin, V. M. Puchkov, and S. V. Finjakov, "Characteristics of HMX combustion waves at various pressures and initial temperatures," *Combust., Expl., Shock Waves*, **34**, No. 2, 170–176 (1998).
15. A. A. Zenin and S. V. Finjakov, "Characteristics of octogen and hexogen combustion: A comparison," in: *Energetic Materials*, Proc. 37th Int. Annu. Conf. of ICT, Karlsruhe, FRG (2006), pp. 154(1)–154(18).
16. N. E. Ermolin and V. E. Zarko, "Modeling of cyclic-nitramine combustion," *Combust., Expl., Shock Waves*, **34**, No. 5, 485–501 (1998).
17. M. W. Beckstead, "Recent progress in modeling solid propellant combustion," *Combust., Expl., Shock Waves*, **42**, No. 6, 623–641 (2006).
18. A. A. Zenin, "Comments to M. W. Beckstead's paper "Recent progress in modeling solid propellant combustion," *Combust., Expl., Shock Waves*, **43**, No. 2, 241–242 (2007).
19. M. W. Beckstead, "Condensed-phase control? Or gas-phase control?" *Combust., Expl., Shock Waves*, **43**, No. 2, 243–245 (2007).
20. G. Lengelle, J. Duterque, and J. F. Trubert, "Physico-chemical mechanisms of solid propellant combustion," in: V. Yang, T. B. Brill, and W. Z. Ren (eds.), *Progress in Astronautics and Aeronautics*, Vol. 185: *Solid Propellant Chemistry, Combustion, and Motor Interior Ballistics*, AIAA, Reston (2000), pp. 287–334.
21. A. F. Belyaev, "Combustion of explosives," *Zh. Fiz. Khim.*, **12**, No. 1, 93–99 (1938).
22. Ya. B. Zel'dovich, "Theory of combustion of propellants and explosives," *Zh. Éksp. Teor. Fiz.*, **12**, Nos. 11/12, 498–524 (1942).
23. G. V. Belov, "Thermodynamic analysis of combustion products at high temperature and pressure," *Propell., Explos., Pyrotechnics*, **23**, 86–89 (1998).
24. A. I. Atwood, T. L. Boggs, P. O. Curran, and D. M. Hanson-Parr, "Burning rate of solid propellant ingredients. Part 1: Pressure and initial temperature effects," *J. Propuls. Power*, **15**, No. 6, 740–742 (1999).
25. A. P. Glazkova, *Data of the Combustion Laboratory of the Institute of Chemical Physics of the Russian Academy of Sciences* (Database entitled "Flame" on combustion of explosives and powders), Mendeleev University of Chemical Technology of Russia (1990–1999).
26. O. P. Korobeinichev, L. V. Kuibida, and V. Zh. Madirbaev, "Investigation of the chemical structure of the HMX flame," *Combust., Expl., Shock Waves*, **20**, No. 3, 282–285 (1984).
27. V. P. Sinditskii, V. Y. Egorshev, A. I. Levshenkov, and V. V. Serushkin, "Combustion of ammonium dinitramide. Part 1: Burning behavior," *J. Propuls. Power*, **22**, No. 4, 769–776 (2006).
28. T. L. Boggs, C. F. Price, D. E. Zurn, et al., "Temperature sensitivity of deflagration rate of HMX," in: *13th JANNAF Combustion Meeting*, CPIA Publ. No. 281, (1976), pp. 45–56.
29. T. P. Parr, T. L. Boggs, C. E. Price, and D. M. Hanson-Parr, "Measurements of temperature sensitivity of HMX burn rates," in: *19th JANNAF Combustion Meeting*, CPIA Publ. No. 366, Vol. 1 (1982), pp. 281–288.
30. V. N. Simonenko, V. E. Zarko, and A. B. Kiskin, "Characterization of self-sustaining combustion of cyclic nitramines," in: *Energetic Materials*, Proc. 29th Int. Annu. Conf. of ICT, Karlsruhe (1998), pp. 169(1)–169(14).
31. A. D. Margolin and A. E. Fogel'zang, "Combustion of tetryl," *Combust., Expl., Shock Waves*, **2**, No. 2, 6–11 (1966).
32. E. B. Washburn and M. W. Beckstead, "Modeling multiphase effects in the combustion of HMX and RDX," *J. Propuls. Power*, **22**, No. 5, 938–946 (2006).
33. V. P. Sinditskii, V. Y. Egorshev, and M. V. Berezin, "Study on combustion of new energetic nitramines," in: *Proc. 32th Int. Annu. Conf. of ICT*, Karlsruhe (2001), Paper No. 59.
34. J. W. Taylor and R. J. Crookes, "Vapour pressure and enthalpy of sublimation of 1,3,5,7-Tetranitro-1,3,5,7-tetraazacyclooctane (HMX)," *J. Chem. Soc., Trans. I*, **72**, 723–729 (1976).
35. A. N. Ali, S. F. Son, B. W. Asay, et al., "High-irradiance laser ignition of explosives," *Combust. Sci. Technol.*, **175**, 1551–1571 (2003).
36. G. N. Kudva and T. A. Litzinger, "Comparison of laser- and pressure-driven thrust response of HMX," *J. Propuls. Power*, **18**, No. 6, 1218–1226 (2002).
37. R. A. Yetter, F. L. Dryer, M. T. Allen, and J. L. Gatto, "Development of gas-phase reaction mechanism for nitramine combustion," *J. Propuls. Power*, **11**, No. 4, 683–697 (1995).
38. P. F. Pokhil, O. I. Nefedova, and A. D. Margolin, "Anomalous dependence of the powder burning rate on initial temperature," *Dokl. Akad. Nauk SSSR*, **145**, No. 4, 860–862 (1962).
39. G. N. Kudva, "A study of lazer and pressure-driven response measurements for propellants at low pressure," Ph. D. Thesis, Pennsylvania State University (2001).
40. J. M. Rosen and C. Dickenson, "Vapor pressures and heats of sublimation of some high melting organic explosives," *J. Chem. Eng. Data*, **14**, 120–124 (1969).

41. R. B. Cundall, T. F. Palmer, and C. E. C. Wood, "Vapor pressures measurements of some organic explosives," *J. Chem. Soc., Faraday Trans. I*, **74**, 1339–1345 (1978).
42. P. G. Hall, "Thermal decomposition and phase transitions in solid nitramines," *Trans. Faraday Soc.*, **67**, No. 3, 556–562 (1971).
43. Yu. A. Maksimov, "Boiling temperature and enthalpy of vaporization of liquid RDX and HMX," *Zh. Fiz. Khim.*, **66**, No. 2, 540–542 (1992).
44. A. P. Korobko, I. V. Levakova, S. V. Krasheninikov, et al., "Solubility of nitrocompounds in an active binder based on polyester urethane rubber and nitroglycerin," *Vooruzhenie. Politika. Konversiya*, No. 5, 69–74 (2002).
45. J.-S. Lee, C.-K. Hsu, and C.-L. Chang, "A study on the thermal decomposition behaviours on PETN, RDX, HNS and HMX," *Thermochim. Acta*, **392, 393**, 173–176 (2002).
46. G. Singh, S. P. Felix, and P. Soni, "Studies on energetic compounds. Part 28: Thermolysis of HMX and its plastic bonded explosives containing estane," *Thermochim. Acta*, **399**, 153–165 (2003).
47. A. A. Paletsky, E. N. Volkov, and O. P. Korobeinichev, "HMX flame structure for combustion in air at a pressure of 1 atm," *Combust., Expl., Shock Waves*, **44**, No. 6, 639–654 (2008).
48. T. P. Parr and D. M. Hanson-Parr, "Thermal properties measurements of solid rocket propellant oxidizers and binder materials as a function of temperature," *J. Energ. Mater.*, **17**, No. 1, 1–47 (1999).
49. Yu. Ya. Maksimov, "Thermal decomposition of RDX and HMX," in: *Theory of Explosives*, Papers of the Mendeleev University of Chemical Technology, Issue 53, Vysshaya Shkola, Moscow (1967), pp. 73–84.
50. J. C. Oxley, A. B. Kooh, R. Szekers, and W. Zhang, "Mechanism of nitramines thermolysis," *J. Phys. Chem.*, **98**, No. 28, 7004–7008 (1994).
51. A. I. B. Robertson, "The thermal decomposition of explosives. — II: Cyclotrimethylenetrinitramine and cyclotetramethylenetetranitramine," *Trans. Faraday Soc.*, **45**, 85–93 (1949).
52. C.E.H. Baun, in: W. E. Garner (ed.), *Chemistry of the Solid State* [Russian translation], Izd. Inostr. Lit., Moscow (1961), pp. 335–353.
53. G. Lengelle, "Thermal degradation kinetics and surface pyrolysis of vinyl polymers," *AIAA J.*, **8**, No. 11, 1989–1996 (1970).
54. A. G. Merzhanov and F. I. Dubovitskii, "Theory of steady combustion of powder," *Dokl. Akad. Nauk SSSR*, **129**, No. 1, 153–156 (1959).
55. V. N. Simonenko, A. B. Kiskin, V. E. Zarko, and A. G. Svit, "Special features of nitramine combustion at atmospheric pressure," *Combust., Expl., Shock Waves*, **33**, No. 6, 685–687 (1997).
56. C.-J. Tang, Y. Lee, and T. A. Litzinger, "Simultaneous temperature and species measurements during self-oscillating burning of HMX," *J. Propuls. Power*, **15**, No. 2, 296–303 (1999).
57. B. V. Novozhilov, *Unsteady Combustion of Solid Propellants* [in Russian], Nauka, Moscow (1973).